

## UNIVERSAL PHOTOGRAMMETRIC APPROACH TO GEOMETRIC PROCESSING OF SPOT IMAGES

Dr. V. Kratky  
Canada Centre for Mapping  
615 Booth Street, Ottawa, Ontario  
CANADA K1A 0E9  
Commission IV

### ABSTRACT

A method for rigorous photogrammetric reconstruction of three-dimensional stereomodels from SPOT images has been developed. The solution is universal as far as applications are concerned and can be implemented both in digital processing systems and in analytical photogrammetric instruments. The images are analyzed in their original raw form (SPOT IMAGE level 1a) corrected in radiometry, but containing no geometric corrections typical of the higher levels of image products. The geometric solution combines the principle of photogrammetric bundle formulation, modified in a time dependent mode, with additional constraints derived from known orbital relations. The inherent accuracy of the geometric reconstruction in a rectangular coordinate system is supported and maintained by a series of rigorous auxiliary transformations between other orbital and cartographic systems involved in the process. Extensive experiments and feasibility tests have proven the viability and good accuracy of the formulation.

### INTRODUCTION

Basic information on the SPOT satellite mission, its goals and technical parameters is available in numerous publications; here we may refer to Chevrel, Weill (1981). To utilize the SPOT potential in the context of cartography and photogrammetry, that is with a special emphasis on geometry, considerable research has been carried out especially in France, but also in other countries, as demonstrated, e.g., by Toutin (1985), Guichard et al. (1987), Denis (1987), Salge et al. (1987), Simard (1987), Cooper et al. (1987). Parallel efforts have also been directed at adaptation of existing on-line analytical photogrammetric instruments and their software to accurate geometric evaluation of SPOT imagery, as reported by de Masson d'Autume (1980), Egels (1983), Dowman, Gagan (1985), Konecny et al. (1987) and Kratky (1987,1988). This paper belongs to the latter category and is based on a rigorous approach intended to have a universal potential for applications even in a fully digital environment.

### BACKGROUND INFORMATION

The orbital geometry, as related to this photogrammetric approach, was described in detail by Kratky (1987). Here, only a summary is presented. The SPOT1 satellite is placed on a close-to-circular elliptical orbit defined by Keplerian motion, with the centre of earth mass in one its foci. Even though the numeric eccentricity of the orbit is very low,  $E=0.00103919$ , the corresponding linear eccentricity is appreciable, displacing the focus of the ellipse from its centre by about 7.5 km. The inclination of the orbital plane from the equator  $i = 98.77^\circ$  determines the top T of the orbital track on the earth ellipsoid. The nominal orbit is expected to maintain its perigee there. Axes A, B of the nominal orbital ellipse can be derived from values of flying altitudes for perigee and apogee, updated and publicized from time to time by SPOT IMAGE. For SPOT traveled angle  $\tau$  measured from the top of the orbit, the geocentric radii  $r$  and  $R$  of the

ground and orbital SPOT positions, respectively, and variable flying altitude  $h = R-r$  can all be computed as functions of this angle. If the perigee does not coincide with the top of the orbit, an angular offset for should be considered in computations.

Time  $t$  is the only independent variable in our orbital relations and one should be able to readily convert  $\tau$  into  $t$  and vice versa. Because of the Keplerian character of the orbit the angular velocity  $\omega_s$  of the satellite is variable, being highest at the perigee and lowest at the apogee. Variable radius vector  $R$  describes a constant area in unit time and, thus, the instantaneous value of  $\omega_s$  is indirectly proportional to  $R^2$ . Consequently, traveled angle  $\tau$  is not directly proportional to the elapsed time  $t$ . With reference to Kratky (1987),  $\tau$  can rigorously be converted into or derived from time  $t$  measured from the perigee, and a rigorous conversion is also readily available for the transition from  $t$  to  $\omega_s$ .

While the SPOT satellite travels, the earth revolves and both these angular changes combine in a composite motion which causes the satellite ground track gradually to deviate from the nominal plane of the orbit. Resulting change  $\lambda_E$  of geographic longitude is proportional to time  $t$  and to the angular velocity  $\omega_E$  of the earth rotation:  $\lambda_E = \omega_E t$ . In the context of our analysis, the composite motion of  $\tau(t)$  and  $\lambda_E(t)$  can be fully assigned to the satellite, as if it orbited around a stationary earth. With reference to Kratky (1973), the effect of traveled angle  $\tau$  can be expressed in terms of geocentric latitude  $\psi$ , reference longitude  $\lambda_s$  measured from the top of orbit and constant angle  $\epsilon = i - 90^\circ$

$$\sin\psi = \cos\epsilon\cos\tau \quad , \quad \tan\lambda_s = \tan\tau/\sin\epsilon \quad , \quad \lambda = \lambda_s + \lambda_E \quad . \quad (1)$$

Geographic latitude  $\phi$  is derived from  $\psi$  by  $\tan\phi = a^2\tan\psi/b^2$ , where  $a$ ,  $b$  represent the semimajor and semiminor axes of the GRS 80 international reference ellipsoid. The satellite position is defined in terms of various polar coordinates  $\tau$ ,  $\lambda_E$ ,  $R$ ,  $\psi$ ,  $\lambda$ ,  $R$  or  $\rho$ ,  $\sigma$ ,  $R$  for any given time  $t$

$$t \begin{array}{l} \longrightarrow \tau, \lambda_E \\ \longrightarrow \psi, \lambda, R \\ \longrightarrow \rho, \sigma, R \end{array} \quad . \quad (2)$$

Polar coordinates can then be converted into rectangular geocentric coordinates as needed.

## COORDINATE SYSTEMS

Several coordinate systems are necessary to apply photogrammetric formulations in the context of orbital and geodetic conditions. They are used to provide a rigorous link between the photogrammetric model, orbit and the reference ellipsoid, as needed in the implementation of the solution.

### Photogrammetric Coordinates

IMG ( $x',y'$ ) - Image Coordinates. Input image coordinates are represented either by the pixel/scanline positions in the digital image record or by corresponding positions measured in transparencies reproduced as a raw image with no geometric corrections involved in the process. In either case the position of an image detail is converted into ideal image coordinates ( $x',y'$ ) with their origin set to the centre pixel of the centre scanline, that is to the centre of the corresponding transparency. This is done in the process of inner orientation.

PHG (U,V,W) - Photogrammetric Coordinates. All photogrammetric relations are expressed in a geocentric rectangular system of coordinates defined with respect to the nominal plane of the left orbit as determined by its expected equator crossing, e.g.,  $\lambda = 93.174^\circ$  for track #305. The U-axis is normal to the orbital plane while W-axis deviates from the top of orbit by angle  $\tau_0$  computed for the centre of the corresponding ground scene, as shown below.

MDL (X,Y,Z) - Model Coordinates. In order to achieve a good numerical stability of photogrammetric computations, model X,Y,Z coordinates are obtained from PHG coordinates by their scaling to the level of image coordinates, that is by equating the flying height with the focal length of the HRV imaging sensor and by setting their origin close to one of the projection centres. Hence, the IMG and MDL coordinate ranges closely correspond to each other.

#### Object Coordinates

UTM (E,N,h) - Universal Transverse Mercator Coordinates. Ground control points for topographical mapping in Canada are available in standard UTM coordinates of easting E and northing N in a system of  $6^\circ$  wide zones related to the regional reference ellipsoid (Clarke 1866) which represents current North American Datum NAD 27. Heights h are related to the local geoid.

GEO ( $\Phi, \Lambda, H$ ) - Geographic Coordinates. They are represented by geographic latitude  $\Phi$  and longitude  $\Lambda$ , supplemented by ellipsoidal height H measured in the normal to the local surface. In conversions to rectangular coordinates geocentric latitude  $\psi$  is used as an alternative to geographic latitude  $\Phi$ . Geographic coordinates are related to a chosen reference ellipsoid, which can be defined regionally (NAD 27) or internationally (GRS 80). The relative orientation and offset of both ellipsoids must be known and considered in coordinate conversions.

GCP - Geocentric Coordinates in Polar Orientation. This coordinate system is geocentric with vertical axis going through the pole and another axis defined by the reference longitude of the related geographic system GEO.

#### Orbital Coordinates

ORB (o,o,r) - Basic Orbital Coordinates. This is a polar coordinate system used mainly for ground points and expressing a geocentric position vector by length r and two orbital angles  $\rho, \sigma$  defined as consecutive rotations along and across the orbital plane, respectively.

CMP ( $\tau, \lambda_E, R$ ) - Composite Orbital Coordinates. This polar coordinate system is used to describe the composite SPOT position vector by geocentric distance R and angles  $\tau, \lambda_E$  which are rotations about axes not perpendicular to each other. The latter angle represents the effect of the earth rotation, possibly extended by a longitudinal displacement of an orbit.

#### Coordinate Transformations

Transformation algorithms and computer subroutines were developed to perform all needed two-way conversions among the systems. Some of the transformations are trivial (polar to rectangular conversions), others may be more involved but are still straight forward (spherical relations), while a few of them (with ellipsoidal relations) cannot be implemented directly and require iterative refinement. An example in the Appendix to this paper illustrates a typical transformation between spherical coordinates.

## PHOTOGRAMMETRIC SOLUTION

### Basic Concepts

In a rigorous system of geometric processing SPOT image information should preferably be analyzed in its original form which is not affected and biased by any spatial changes caused by resampling, modified display or photo reproduction of images. The imagery on input should be represented by raw image data containing no corrections except for those improving their radiometric rendition (SPOT IMAGE level 1a). This condition applies to both major classes of procedures operating either directly on digital images, or on their photoreproduced transparencies in on-line photogrammetric systems. The analytical reconstruction of geometric relations should always be carried out in three-dimensional Cartesian space with all related tasks of individual image rectification or resampling left to follow in subsequent operations. Only then can they be properly controlled by the previously established rigorous mathematical model of geometric relations.

The three-dimensional character of the photogrammetric formulation allows to consider, in a rigorous way, all physical aspects of satellite orbiting and of the earth imaging, as well as the proper conditions of the time-dependent intersection of corresponding imaging rays in the model space. The orbital parameters, either predicted or extracted from SPOT ephemeris data are not applied in an absolute way. Potential orbital perturbations due to the earth's gravitational field and accumulated irregularities in the control of the orbit are taken into account by allowing the SPOT orbital segment, corresponding to the viewed ground scene, to be additionally shifted with respect to its expected nominal position, in order to find the best fit for the image projecting rays with given ground control points and to provide a good intersection of all corresponding projecting rays. Thus, the resulting reference SPOT position  $\tau_0$  for the ground scene centre can move along the orbit and the orbit can also be offset in geographic longitude  $\lambda$ . Simultaneously, a proper mathematical model for the imaging sensor's attitude variations is defined or modified in the process. It is worth mentioning that in the solution concepts there is no absolute need for using additional information, such as from SPOT IMAGE supplemental data file, however, if available, it is useful to be used either directly or in order to assess the practicality of a more refined solution, as mentioned later.

### Initial Conditions

The PHG coordinate system coincides with the nominal plane of the left SPOT orbit, with one axis displaced from the top of orbit by reference angle  $\tau_0$  which defines the SPOT position for the centre of the ground scene with corresponding elevation  $h$ . The annotation of raw imagery provides the geographic coordinates of the scene centre, the orbit number and the view angle of the sensor. All these values may not be fully consistent with the orbital geometry since the given view angle does not necessarily reflect the local attitude of the sensor. Consequently, only the remaining values are used to derive reference angle  $\tau_0$ , that is the position from which the scene centre is seen from the given track. The analytical algorithm briefly described here is a typical example of many complex dynamic relations considered in rigorous photogrammetric solutions.

1. The coordinates of the ground scene centre are checked and refined by direct comparison of the image with a map, yielding geographic latitude  $B$  and longitude  $L$ , and the orbit number  $m$  is converted into track number  $n$

$$n = \text{MOD}(26(370-m)+1, 369) = \text{MOD}(9621-26m, 369) \quad ,$$

where  $\text{MOD}(j,k)$  represents division of  $j$  modulo  $k$ .

2. A series of operations is performed to determine the composite longitude of the scene due to SPOT travel and earth revolution

track equator crossing  $L_0$  for n  

$$L_0 = 389.759^\circ + (1-n)360/369 \quad ,$$
longitude difference  $L_{TQ}$  from top of orbit to equator  

$$L_{TQ} = 90^\circ + \omega_E F_t(90^\circ) \quad ,$$
longitude for top of orbit  $L_T$   

$$L_T = L_0 - L_{TQ} \quad ,$$
composite longitude  $L_C$  from top of orbit to scene centre  

$$L_C = L - L_T \quad .$$

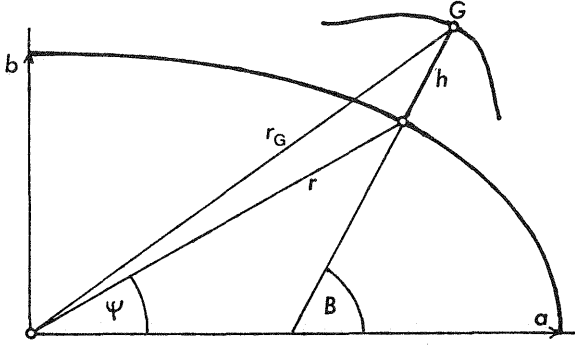


Fig. 1 Geocentric Latitude

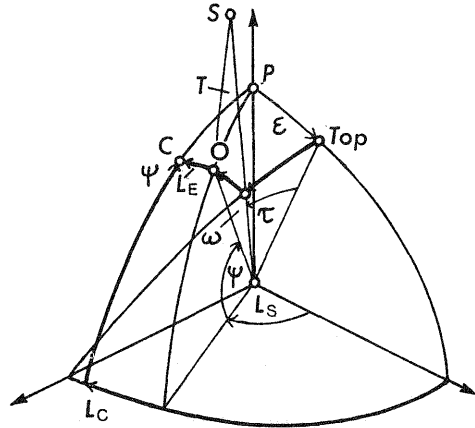


Fig. 2 Spherical Relations

3. With reference to Fig. 1, the scene geographic latitude B is converted into geocentric latitude  $\psi$  and geocentric distance  $r_G$  for ground point G is computed. The angular difference between  $\psi$  and the radius vector for G is negligible for any practical elevations h

$$\tan \psi = b^2 \tan B / a^2$$

$$r^2 = a^2 b^2 / (a^2 \sin^2 \psi + b^2 \cos^2 \psi)$$

$$r_G = r + h$$

4. Fig. 2 represents only angular relations with no regard to distances. Point C represents the real, composite spherical position of the scene defined by rotations  $L_C, \psi$ . Without the earth rotation effect the scene would be located at point O and this position can be defined either by geographic rotations  $L_S, \psi$  or by orbital rotations  $\tau, \omega$ . The relation between these two pairs of coordinates GEO-ORB:  $L_S, \psi \longleftrightarrow \tau, \omega$  is a straight forward transformation (see Appendix), however, in order to derive position O we have to subtract from C the effect of  $L_E$ , which is a function of so far unknown spot traveled angle  $\tau$ . The solution is obtained by iterations, with the use of  $F_t$  of Eq. (4) as follows

Estimate  $\omega = 0$   
Estimate  $\tau$  from Eq. (1):  $\cos \tau = \sin \psi / \cos \epsilon$   
Repeat  
 $\tau_i = \tau$   
 $L_S = L_C - \omega_E F_t(\tau_i)$   
GEO-ORB:  $L_S, \psi \longleftrightarrow \tau, \omega$   
Until  $\tau_i = \tau$

5. Finally, we calculate SPOT geocentric distance R for reference position  $\tau_0 = \tau$  and tilt T corresponding to orbital angle  $\tau$

$$R = A(1-E^2)/(1+E \cos \tau)$$

$$\tan T = \sin \omega / [(R/r_G) - \cos \omega]$$

## Inner Orientation

In the process of inner orientation coordinates  $x'$  are adjusted to the physical length of the sensor's linear CCD array ( $6000 \times 13 \mu\text{m} = 78 \text{ mm}$ ). Coordinates  $y'$  are assuming the same scale, however, during photogrammetric computations they are merely used as a measure of time which is the primary independent parameter in our solution. Their conversion into time  $t$  is possible by comparing the image  $y'$ -range with the time interval needed to make the 6000 consecutive scans in the scene ( $6000 \times 1.504 \text{ ms} = 9.024 \text{ s}$ ). The scale of the transparency is not important. Inner orientation will fit the measured corners of the raw image with an ideal square pattern of fictitious fiducial marks, with coordinate origin in their centre and a separation of 78 mm in both directions. Affine or bilinear transformation converts measurements into ideal IMG coordinates  $(x', y')$ .

The conversion of  $y'$  into time interval  $\Delta t$  is implemented with the use of a known constant rate  $c_t = dt/dy' = 9.024/78 = 0.11569 \text{ s/mm}$  which yields

$$\Delta t(y') = - c_t y' \quad .$$

Traveled angle  $\tau$  can be derived directly from  $y'$  by  $\tau = \tau_0 - c_\tau y'$  where

$$c_\tau = d\tau/dy' = (d\tau/dt)(dt/dy') = \omega_s c_t \quad , \quad (3)$$

or rigorously, with direct conversions  $\tau = F_\tau(t)$  and  $t = F_t(\tau)$  (see Kratky, 1987) applied by

$$\tau = F_\tau(F_t(\tau_0) + \Delta t(y')) \quad . \quad (4)$$

## Formulation of the Photogrammetric Solution

The principle of an extended bundle formulation is applied to both ground control points and intersection points. The fact that the spatial bundles of reconstructed image rays are restricted to a plane, and the field of sensor's view is very narrow, results in a high correlation between the projection centre displacement and sensor's tilt in the same direction. These pairs of unknowns cannot be separated in a standard bundle solution and the inherent singularity of the solution must be avoided by inclusion of additional constraints derived from known orbital relations. The constraining values can be either estimated from expected nominal orbits or obtained from supplemental data file available in digital image tapes. There are numerous possibilities of including this type of information into a constrained photogrammetric solution and several variants were tested before the present approach was adopted.

The total number of unknown parameters of the solution is 26, defined in the following way. 12 standard orientation elements are represented by the reference positions  $(X, Y, Z)_0$  of SPOT projection centres and the reference attitude elements  $(\alpha, \phi, \omega)_0$  of sensors, all corresponding to the centre of images ( $x'=y'=0$ ). Additional 12 parameters are linear and quadratic rates of change for attitude elements as modeled by polynomials dependent on  $y'$ . Finally, an auxiliary change of image scale in the direction of scanlines is allowed by defining corrections to the nominal focal length  $f$  of individual sensors (2 unknowns).

Weighted constraints are formulated to keep the  $\tau, \lambda$  orbital position of the left sensor, the  $\Delta\tau, \Delta\lambda$  relative position of the stereo related orbits and their geocentric distances  $R$  - all for the image centres - within statistical limits specified at the outset of the solution. This adds six constraining conditions to the solution.

In order to keep projection centres moving only along appropriate elliptical orbital segments 12 absolute constraints are enforced. The segments must rigorously correspond to the reference position  $(X,Y,Z)_0$ , as currently known from the iterative process. Current coordinates of the projection centre are used to find the new, coinciding orbit and SPOT position, displaced by  $d\tau$  and  $d\lambda$  with respect to the initial reference position in the nominal orbit. Then we calculate the needed linear and quadratic rates of change in  $X,Y,Z$  which are used as given, absolutely accurate values.

The attitude model can be simplified by disregarding the quadratic terms when judged appropriate, or by substituting for them values from the supplemental data file. In this instance, the number of unknowns drops by six to the total of 20. Accordingly, the minimum practical number of control points needed to support a solution varies between 5 and 9.

The formulation of a bundle solution is expanded by the effect of the time-dependent parameters. For the analytical detail on modifications of a standard approach as implemented in our solution, we refer to Kratky (1987). In collinearity equations the projection centres are represented by quadratic polynomials

$$X_c = X_0 + y' \dot{X} + y'^2 \ddot{X} \quad , \quad Y_c = Y_0 + y' \dot{Y} + y'^2 \ddot{Y} \quad , \quad Z_c = Z_0 + y' \dot{Z} + y'^2 \ddot{Z} \quad (5)$$

with rates  $\dot{X}$ ,  $\ddot{X}$ ,  $\dot{Y}$ ,  $\ddot{Y}$ ,  $\dot{Z}$ ,  $\ddot{Z}$  computed for the current reference SPOT position and similarly, the time dependent rotation matrix is defined as  $T_t = F_T(y') = F(\alpha, \phi, \omega)$  with

$$\alpha = \alpha_0 + y' \dot{\alpha} + y'^2 \ddot{\alpha} \quad , \quad \phi = \phi_0 + y' \dot{\phi} + y'^2 \ddot{\phi} \quad , \quad \omega = \omega_0 + y' \dot{\omega} + y'^2 \ddot{\omega} \quad . \quad (6)$$

Since photocoordinate  $y'$  is used only as a measure of time  $t$ , individual scanlines (with  $y'=0$ ) determine planar sheaves of projecting rays which are then subjected to standard orthogonal transformations represented here by  $(x \ y \ z)^T = T_t (x' \ 0 \ -f)^T$ .

## CARTOGRAPHIC ASPECTS

The strength of a stereophotogrammetric approach in geometric satellite image processing results from the fact that spatial relations are formed and solved in a three-dimensional rectangular system, so avoiding or circumventing some of the complexities of curvilinear reference systems. However, ground control information has to be supplied from an external cartographic system and, vice versa, the reconstructed photogrammetric model has to be interpreted in terms of this external system.

A rigorous process of mutual cartographic - photogrammetric referencing was developed to suit the regional conditions in Canada. The following transformations are needed:

- h-H : conversion of geoidal heights  $h$  to NAD 27 ellipsoidal heights  $H$ ;
- UTM-GEO: conversion of UTM coordinates to geographic coordinates  $\Phi, \Lambda$  in NAD 27;
- GEO-GCP: conversion of geographic to geocentric coordinates in NAD 27;
- GCP-GCP: offset of geocentric NAD 27 coordinates to international system GRS 80;
- GCP-GEO: conversion of geocentric to geographic coordinates in GRS 80;
- GEO-ORB: conversion to polar orbital coordinates  $\rho, \sigma, r$  in the chosen nominal orbital plane;
- ORB-PHG: conversion to geocentric coordinates  $U, V, W$  oriented with respect to expected SPOT position  $\tau_0$ ;
- PHG-MDL: translation and scaling into model coordinates  $X, Y, Z$ .

A reversed sequence of the above steps will transform photogrammetric MDL coordinates back to UTM system and to geoidal heights in the NAD 27 system.

#### ON-LINE IMPLEMENTATION

Two major aspects must be considered when applying the SPOT solution in an on-line photogrammetric environment: 1. the control of image positioning must cope with dynamic changes in the position and attitude of the sensor and still retain its needed real-time performance; 2. in the continuous compilation mode, the elevations entered on input must be defined with respect to the curved ellipsoidal or geoidal surface.

A detailed analysis of these and other on-line aspects of processing SPOT images and a description of the way in which the problems are resolved in our solution is presented in Kratky (1988). Here, only two main conclusions are briefly mentioned. The positioning control is feasible and efficient even with straight forward IMG-MDL and MDL-IMG transformations of coordinates when the algorithms are streamlined to shorten the iteration cycle inherent in the latter transformation and modified to speed up the construction of orthogonal matrices. With the use of single precision arithmetics the duration of the positioning real-time cycle is 2-3 ms with the support of DEC VAX 750 microcomputer. The cycle has a satisfactory frequency of about 50 Hz even for PDP 11/45 minicomputer supporting the NRC ANAPLOT-I plotter on which the experiments and tests have been conducted. The control of ellipsoidal heights in the plotter input has been handled through a 9-term polynomial function of 3rd degree  $Z = F_z(x', y', h)$  which provides a fast and accurate transformation with maximum errors well below 1 m even within a 4 km range of elevations.

#### PRACTICAL RESULTS

The solution for stereo images usually requires 3-6 iterations and yields all parameters needed for any further geometric control and processing, as well as their stochastic evaluation. A practical solution is obtained with a minimum of 5-9 ground control points, depending on the degree of the polynomial SPOT attitude model. The inner accuracy of the algorithm as tested by fictitious data, ensures a submicrometre least squares fit of image data, and RMS ground errors are within the range of 0.2 to 0.3 m for both planimetry and heights, when base-to-height ratio is around 1.

Several tests were conducted with real imagery. Three individual SPOT scenes were processed in a single image solution yielding RMS errors of 6-7 m in X or Y coordinates, based on comparison with about 80 check points. The only stereopair tested so far consisted of images taken four orbits apart in August 1987, with view angles  $+27.89^\circ$  and  $+7.31^\circ$  and with a very poor base-to-height ratio of 0.4. A solution supported by nine control points and using quadratic modeling of position and attitude variations provided a least square fit with standard unit error of 6.4  $\mu\text{m}$ . Resulting RMS discrepancies in control points were

X ... 2.4 m , Y ... 2.4 m , Z ... 8.2 m ,

while 63 independent check points yielded RMS errors

X ... 5.1 m , Y ... 6.2 m , Z ... 13.3 m .

Residual RMS Y-parallaxes were 4.5 m at ground scale. The relatively high elevation errors are within limits expected from the unfavourable b/h ratio.

Interestingly, when the model of attitude variations was simplified to a linear form, the solution with only six control points retained the performance of the previous example. Standard error of unit weight was

increased to 8  $\mu\text{m}$ , the control point RMS discrepancies were changed to  
 X ... 3.2 m , Y ... 0.8 m , Z ... 10.7 m ,  
 while RMS errors in 65 check points showed a slight improvement in Z  
 X ... 4.9 m , Y ... 6.3 m , Z ... 12.2 m .  
 Obviously, in this case the need for a quadratic attitude model was not warranted.

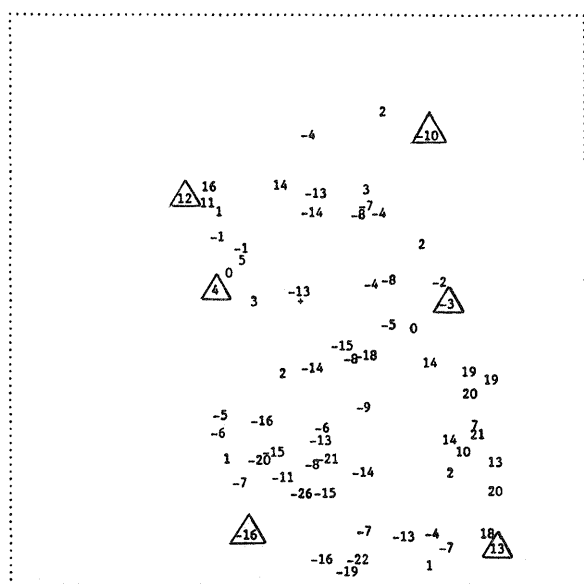


Fig. 3 Height Residuals

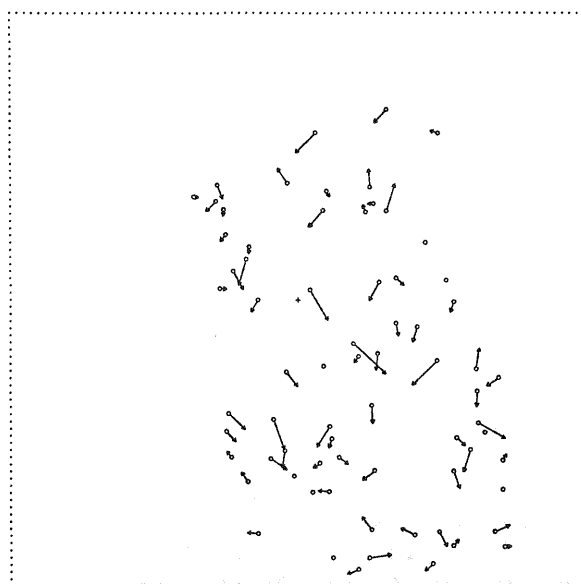


Fig. 4 Planimetric Residuals

Figs. 3 and 4 show the values and distribution of height errors (in m) and planimetric error vectors, respectively, for 6 control points and 65 check points used in the last example of solution. Control points are marked by triangles. The point positions are plotted as they appear in the left SPOT image. Its overlap with the right image is almost 100%. Obviously, the configuration pattern of control points is not ideal to cover sufficiently the whole area of image overlap and to provide optimal geometric conditions for the solution.

REFERENCES

Chevrel, M. and G. Weill, 1981. The SPOT Satellite Remote Sensing Mission. Photogrammetric Engineering and Remote Sensing, 47(8): 1163-1171.  
 Cooper, P.R., D.E. Friedmann and S.A. Wood, 1987. The Automatic Generation of Digital Terrain Models from Satellite Images by Stereo. Acta Astronautica 15(3):171-180.  
 Denis, P., 1987. Applications métriques de la stéréoscopie latérale de SPOT. Actes du Colloque International "SPOT1 - Utilisation des images, bilan, résultats", CNES, Paris.  
 Downman, I.J. and D.J. Gagan, 1985. Application Potential of SPOT Imagery for Topographical Mapping. Advanced Space Research, 5(5):73-79.  
 Egels, Y., 1983. Amélioration des logiciels TRASTER: restitution d'images à géométrie non conique. Bull. Inf. IGN, 1983(2):19-22.  
 Guichard, H., G. Ruckebusch, E. Sueur and S. Wormser, 1987. Stéréorestitution numérique SPOT: une approche originale des images épipolaires et de mise en correspondance. Actes du Colloque International "SPOT1 - Utilisation des images, bilan, résultats", CNES, Paris.  
 Konecny, G., P. Lohmann, H. Engel and E. Kruck, 1987. Evaluation of SPOT Imagery on Analytical Photogrammetric Instruments. Photogrammetric Engineering and Remote Sensing, 53(9):1223-1230.

- Kratky, V., 1973. Cartographic Accuracy of ERTS. Photogrammetric Engineering, 40(2):203-212.
- Kratky, V., 1987. Rigorous Stereophotogrammetric Treatment of SPOT Images. Actes du Colloque International "SPOT1 - Utilisation des images, bilan, résultats", CNES, Paris.
- Kratky, V., 1988. On-Line Aspects of Stereophotogrammetric Processing of SPOT Images. International Archives of Photogrammetry and Remote Sensing, 27(2), ISPRS, Kyoto.
- de Masson d'Autume, M.G., 1980. Le traitement géométrique des images de télédétection. Annales des Mines, 1980(2):53-62.
- Salge, F., M.J. Roos-Josserand and P. Campagne, 1987. SPOT, un outil de saisie et de mise à jour pour la base de données cartographiques de l'IGN. Actes du Colloque International "SPOT1 - Utilisation des images, bilan, résultats", CNES, Paris.
- Simard, R., 1987. Modélisation numérique du terrain avec les données SPOT et applications aux sciences de la Terre. Actes du Colloque International SPOT1 - Utilisation des images, bilan, résultats", CNES, Paris.
- Toutin, T., 1985. Analyse mathématique des possibilités cartographiques du système SPOT. Thèse du doctorat, Ecole Nationale des Sciences Géographiques. Paris.

## APPENDIX

Geographic to Orbital Transformation  $(\lambda, \phi) \longmapsto (\rho, \sigma)$

This is an example of a spherical transformation in which geographic latitude  $\phi$  and geocentric latitude  $\psi$  are identical. Auxiliary coordinate system XYZ defines rotations  $\varepsilon, \rho, \sigma, \lambda, \psi$  as marked in Fig. 5. Longitude  $\lambda$  is measured from the reference meridian passing through the top of orbit T. Individual matrices are

$$T_{\varepsilon} = \begin{bmatrix} 1 & 0 & 0 \\ 0 & \cos\varepsilon & \sin\varepsilon \\ 0 & -\sin\varepsilon & \cos\varepsilon \end{bmatrix} \quad T_{\rho} = \begin{bmatrix} \cos\rho & 0 & \sin\rho \\ 0 & 1 & 0 \\ -\sin\rho & 0 & \cos\rho \end{bmatrix}$$

$$T_{\sigma} = \begin{bmatrix} 1 & 0 & 0 \\ 0 & \cos\sigma & -\sin\sigma \\ 0 & \sin\sigma & \cos\sigma \end{bmatrix} \quad T_{90-\lambda} = \begin{bmatrix} \sin\lambda & -\cos\lambda & 0 \\ \cos\lambda & \sin\lambda & 0 \\ 0 & 0 & 1 \end{bmatrix}$$

$$T_{90-\phi} = \begin{bmatrix} \sin\phi & 0 & \cos\phi \\ 0 & 1 & 0 \\ -\cos\phi & 0 & \sin\phi \end{bmatrix} .$$

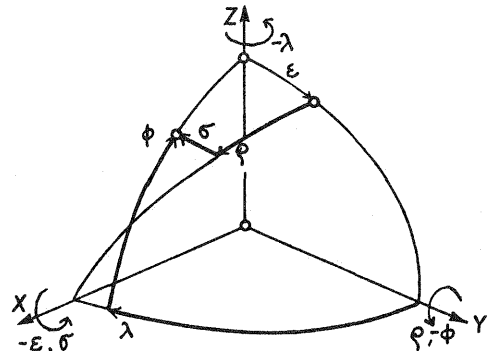


Fig. 5 Spherical relations

The relation between the two systems is easy to derive from two sets of consecutive rotations which displace Z-axis  $Z = (0 \ 0 \ 1)^T$  from P to G. In matrix notation we can write  $T_{\rho} T_{\sigma} Z = T_{\varepsilon}^T T_{90-\lambda} T_{90-\phi} Z$ , which produces vectors

$$\begin{pmatrix} \sin\rho \cos\sigma \\ -\sin\sigma \\ \cos\rho \cos\sigma \end{pmatrix} = \begin{pmatrix} \sin\lambda \cos\phi \\ \cos\varepsilon \cos\lambda \cos\phi - \sin\varepsilon \sin\phi \\ \sin\varepsilon \cos\lambda \cos\phi + \cos\varepsilon \sin\phi \end{pmatrix} ,$$

from which we derive

$$\begin{aligned} \tan\rho &= \sin\lambda / (\sin\varepsilon \cos\lambda + \cos\varepsilon \tan\phi) , \\ \sin\sigma &= \sin\varepsilon \sin\phi - \cos\varepsilon \cos\lambda \cos\phi . \end{aligned} \quad (7)$$

A modification of the above matrix product to  $T_{90-\lambda} T_{90-\phi} Z = T_{\varepsilon} T_{\rho} T_{\sigma} Z$  will produce vectors for the inverse transformation of  $\rho, \sigma$  into  $\lambda, \phi$ .